

a V^{N-1} type. On the other hand, the V^N state $|k_0\rangle$ is unmodified and gives the correct asymptotic behavior for a scattered electron. Thus, the two divergent boundary conditions are resolved by the usage of two basis sets in the same diagram.

We have given several concrete examples for which the method of the multiple basis set can be

employed to sum exactly classes of diagrams to infinite order. In a larger scope the same method may also be fruitfully used to make approximate summations. This method of using multiple basis set should greatly extend the power and usefulness of the BG-theory approach in an even wider range of atomic calculations.

*Work partially supported by NASA and NSF.

†Formerly R. T. Pu.

¹H. P. Kelly, Phys. Rev. **131**, 684 (1963); **136**, B369 (1964); see also O. Sinanoğlu and K. A. Brueckner, *Three Approaches to Electron Correlation in Atoms* (Yale U.P., New Haven, 1970).

²E. S. Chang, R. T. Pu, and T. P. Das, Phys. Rev. **174**, 1 (1968).

³R. T. Pu and E. S. Chang, Phys. Rev. **151**, 31 (1966).

⁴E. S. Chang and M. W. C. McDowell, Phys. Rev. **176**, 126 (1968); T. Ishihara and R. T. Poe, in *Proceedings of the Sixth International Conference on the Physics of Electronic and Atomic Collisions* (MIT Press, Cambridge, Mass., 1969).

⁵N. C. Dutta, T. Ishihara, C. Matsubara, and T. P. Das, Phys. Rev. Letters **22**, 8 (1969).

⁶A. A. Abrikosov, L. P. Gorkov, and I. E. Dzyaloshinski, *Methods of Quantum Field Theory in Statistical Physics* (Prentice-Hall, Englewood Cliffs, N. J., 1963).

⁷J. Goldstone, Proc. Roy. Soc. (London) **A239**, 267 (1957).

⁸S. Huzinaga and C. Arnau, Phys. Rev. A **1**, 2285 (1970); H. J. Silverstone and M. L. Tin, J. Chem. Phys. **49**, 2076 (1968).

⁹E. S. Chang, R. T. Pu, and T. P. Das, Phys. Rev. **174**, 16 (1968).

¹⁰P. W. Langhoff, R. P. Hurst, and M. Karplus, J. Chem. Phys. **44**, 505 (1966).

Brueckner-Goldstone Many-Body Perturbation Calculation of Helium Photoionization*

T. Ishihara and R. T. Poe†

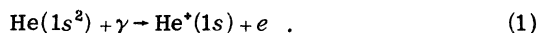
Physics Department, University of California, Riverside, California 92502

(Received 12 February 1971)

A calculation is carried out within the framework of the Brueckner-Goldstone many-body perturbation approach for the photoionization of helium. In particular, we have utilized a newly developed technique of multiple basis sets to circumvent the difficulty of evaluating the singular integrals which appear in the important final-state correlation. This technique also enables us to achieve considerable calculational simplicity, reducing the final evaluation to only two diagrams. Our result agrees well with the accurate experimental data of Samson.

I. INTRODUCTION

In the past few years, the Brueckner-Goldstone (BG) many-body perturbation-theory (MBPT) approach has been successfully applied to a diverse number of atomic calculations.¹⁻³ Recently, Chang and McDowell,⁴ and later Ishihara and Poe,⁵ applied the BG approach to photoionization problems in Li atom. Although, in general, good agreement is obtained, a detailed test of the applicability of the BG approach for the photoionization problem is made difficult by the considerable uncertainty in the experimental data in the lithium case. For this reason we report the result of the BG calculation of the photoionization process in helium:



There are several interesting features in the

present calculation. First, with the existence of very accurate experimental data,⁶ this calculation serves as a critical assessment of the accuracy and usefulness of the BG approach for general photoionization problems. From a calculational point of view, it is also an ideal test case because of the extreme simplicity of the two-electron helium system. This avoids the redundancy of evaluating a large number of similar diagrams while still preserving the essential features of general photon-atom reactions.

In addition, there exist very important intrashell correlation effects between the two valence electrons in He, a feature which is absent in the Li case. In the conventional MBPT approach, these terms yield a singularity in the summation of intermediate states, making its evaluation quite impracticable. We have circumvented this calcula-

tional difficulty by the technique of the multiple basis set we have developed recently.⁷ Therefore the usefulness of the multiple basis set is also being demonstrated in the present calculation.

In Sec. II, we describe briefly the MBPT approach to the photoionization problems. Important diagrams for the ionization of He are given in Sec. III, and the problem is greatly simplified through the multiple-basis-set technique. In Sec. IV, we give numerical results and discussion.

II. MBPT APPROACH TO PHOTOIONIZATION PROBLEMS

The total Hamiltonian H for an N -electron atom in the external radiation field is given by

$$H = H_0 + H_c + H_\gamma(t) , \quad (2)$$

where

$$H_0 = \sum_{i=1}^N (T_i + V_i) , \quad (3)$$

$$H_c = \sum_{i>j}^N v_{ij} - \sum_i^N V_i , \quad (4)$$

and

$$H_\gamma(t) = \sum_i^N G_i e^{-i\omega t} + \text{c. c.} . \quad (5)$$

T_i is the sum of the kinetic energy and nuclear potential of the i th electron; an arbitrary single-particle potential V_i is to be determined for each specific problem. See Sec. III. $v_{ij} = 1/r_{ij}$ is the electron-electron interaction, and G_i is the dipole interaction on the i th electron.

The time-development operator $U(t, t_0)$ is expanded as

$$U(t, t_0) = \sum_{n=0}^{\infty} \frac{(-i)^n}{n!} \iint_{t_0}^t \dots \int dt_1 dt_2 \dots dt_n \\ \times T(H'(t_1)H'(t_2) \dots H'(t_n)) , \quad (6)$$

where

$$H'(t) = e^{iH_0 t} [H_c + H_\gamma(t)] e^{-iH_0 t} e^{-\eta|t|} , \quad (7)$$

with $\eta \rightarrow +0$ and T being Wick's chronological operator.

The N -electron eigenfunction Φ_n of the unperturbed system H_0 satisfying

$$H_0 \Phi_n = E_n^0 \Phi_n \quad (8)$$

can be expressed as combinations of Slater determinants of a complete set of single-particle wave functions φ_α generated by

$$(T + V)\varphi_\alpha = \epsilon_\alpha \varphi_\alpha , \quad (9)$$

and lowest N orbitals are occupied in the ground state Φ_0 . Although our perturbation theory is entirely based on this complete set, we will introduce another complete set in Sec. III as a result of partial summation of higher-order terms.⁷

The S matrix for the transition from the ground state Φ_0 to an excited state Φ_f , where several holes and particles exist, is given by

$$S_{f0} = \langle \Phi_f | U(\infty, -\infty) | \Phi_0 \rangle . \quad (10)$$

As is well known, the perturbation expansion of S_{f0} can be represented as a sum of Feynman-like diagrams. Each diagram is decomposed into linked and unlinked parts, and the latter can be factored out to give the expression⁸

$$S_{f0} = \langle \Phi_f | U_L(\infty, -\infty) | \Phi_0 \rangle e^{U_{0c}} . \quad (11)$$

The sum of all the unlinked connected diagrams U_{0c} is shown to be pure imaginary, and we can omit the factor $e^{U_{0c}}$ in the calculation of transition probability.

Consider the ionization process due to a single-photon absorption. Multiphoton processes can be treated similarly. S_{f0} is then given by the sum of linked diagrams of first order in G , with hole and particle lines of Φ_f at the top of the diagrams, e.g., diagrams in Sec. III. After the t integrations of Eq. (6), all these diagrams have a factor $(-2\pi i)\delta(E_f^0 - E_0^0 - \omega)$ which represents the energy conservation in the unperturbed system. However, this may be replaced by the true energy conservation $(-2\pi i)\delta(E_f - E_0 - \omega)$ if we take into account certain interactions in the final state up to infinite order. In the case of single ionization such as Eq. (1), this is given by the self-energy insertion to the hole line in the final state.⁹ Thus

$$S_{f0} = -2\pi i \delta(E_f - E_0 - \omega) T_{f0} . \quad (12)$$

Contribution of each diagram to T_{f0} can be calculated by the usual rules¹⁰ with the exception of a modification of the energy denominator. Because of the time dependence in $H_\gamma(t)$, the denominators become $(E_0^0 - H_0 + \omega + i\eta)$ above the vertex G and $(E_0^0 - H_0)$ below it.³

III. PHOTOIONIZATION OF He

For the process of Eq. (1), the logical choice of the basis set, Eq. (9), of the expansion is the V^{N-1} type defined by

$$(T + \int \varphi_{1s}^*(\vec{r}') v(\vec{r}, \vec{r}') \varphi_{1s}(\vec{r}') d\vec{r}') \varphi_\alpha(\vec{r}) = \epsilon_\alpha \varphi_\alpha(\vec{r}) . \quad (13)$$

This is the Hartree-Fock (HF) equation for the $1s$ state, and in excited states the electron sees one electron in the HF $1s$ orbital. This type of V^{N-1} basis set has been extensively used in calculations involving one-electron excitations.

The zeroth-order term in H_c is given in Fig. 1(a) and describes the usual one-electron picture. In the diagrams, the external dipole interaction G is represented by a wavy line while the electron-electron interaction v is represented by a dotted line. The contribution of this lowest-order dia-

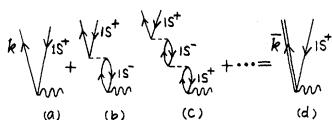


FIG. 1. Diagrams representing zeroth-order contribution to the photoionization and higher-order intrashell self-consistency corrections.

gram to T_{f0} in Eq. (12) is simply

$$T_{1a} = \langle k | G | 1s \rangle \quad (14)$$

There are two diagrams representing the next-order terms. Figure 1(b) contains the first-order electron correlation in the final state while Fig. 2(a) represents the first-order correction to the initial (HF) state of He atom. The contributions of these diagrams are given by

$$T_{1b} = \sum_{k'} \frac{\langle k, 1s | v | 1s, k' \rangle \langle k' | G | 1s \rangle}{\epsilon_{1s} - \epsilon_{k'} + \omega + i\eta} \quad (15)$$

and

$$T_{2a} = \sum_{k'} \frac{\langle 1s | G | k' \rangle \langle k, k' | v | 1s, 1s \rangle}{2\epsilon_{1s} - \epsilon_k - \epsilon_{k'}} \quad (16)$$

These terms are not small and tend to cancel each other. Therefore they should be evaluated accurately. It also turns out that Eq. (15) has a zero in the energy denominator, and it makes accurate numerical integration extremely difficult. The same type of singularity also occurs in other higher-order diagrams, such as those in Figs. 1(c), 2(b), and 2(c). Physically, these diagrams represent the intrashell consistency effects between two valence electrons.

This difficulty is avoided in the calculation by the use of the multiple-basis-set technique we have developed recently.⁷ With this technique, the whole class of diagrams in Figs. 1(a), 1(b), 1(c), and the higher-order terms are exactly replaced by the one simple term shown in Fig. 1(d). The double line in the diagram represents a new basis set $\bar{\varphi}_k$ which satisfies a Schrödinger equation differing from the original one by the addition of an exchange-like self-consistency interaction term,

$$\begin{aligned} [T + \int \varphi_{1s}^*(\vec{r}') v(\vec{r}, \vec{r}') \varphi_{1s}(\vec{r}') d\vec{r}'] \bar{\varphi}_k(\vec{r}) \\ + [\int \varphi_{1s}^*(\vec{r}') v(\vec{r}, \vec{r}') \bar{\varphi}_k(\vec{r}') d\vec{r}'] \varphi_{1s}(\vec{r}) = \bar{\epsilon}_k \bar{\varphi}_k(\vec{r}) \end{aligned} \quad (17)$$

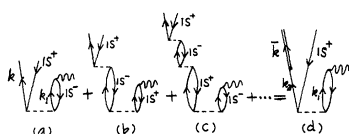


FIG. 2. Diagrams containing first-order correction to the initial state.

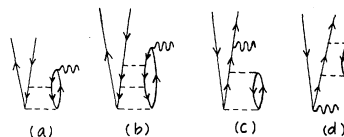


FIG. 3. (a) and (b) EPV diagrams which give rise to the shift of the energy denominator. (c) and (d) Second-order polarization corrections.

Through the same technique, the initial-state correction term Fig. 2(a), and its higher-order self-consistency terms Fig. 2(b), Fig. 2(c), etc. can be summed exactly, yielding another simple diagram as shown in Fig. 2(d). The dot between the double line \bar{k} and the single line k_2 represents an overlapping integral⁷ $\langle \bar{k} | k_2 \rangle$.

Finally, for diagrams in Fig. 2, there also exist important higher-order hole-hole ladder terms as illustrated in Figs. 3(a) and 3(b). These can be included in the calculation of Fig. 2(d) by the use of the shifted energy denominator.¹ Figures 3(c) and 3(d) represent core-polarization effects in the initial and final states. These two effects tend to cancel each other and are concluded to be small in the Li case.⁵ Thus they are not included in this calculation.

With the use of the multiple basis set, we are able to circumvent the difficulty arising from the singularity of the intrashell diagrams. With the same technique we also achieved considerable calculation simplicity. The large number of diagrams which occur in the conventional BG approach [those in Figs. 1, 2, and 3(a), 3(b), ...] are reduced to only two simple diagrams. Contributions T_{1d} and T_{2d} from these diagrams and the cross-section formula are given by (in atomic units)

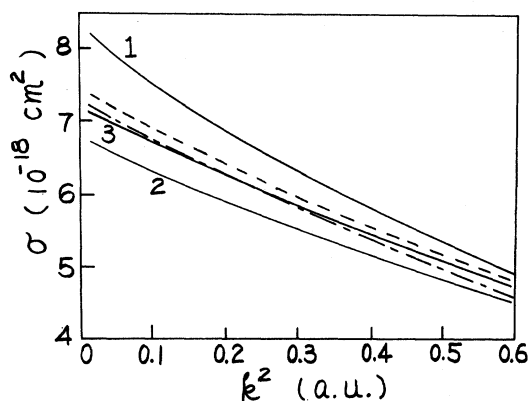


FIG. 4. Comparison of theory and experiment for helium photoionization cross sections. Curve 1 is from diagram 1(a), curve 2 is from 1(d), and curve 3 is from 1(d) plus 2(d). Dotted line is the dipole-length calculation of Stewart and Webb, dot-dash curve is the experimental result of Samson.

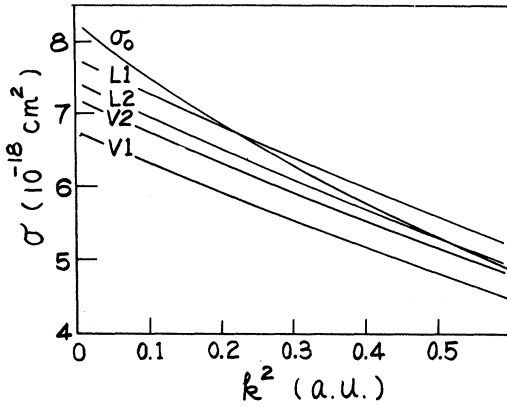


FIG. 5. Comparison of length and velocity formulas. σ_0 is the cross section from diagram 1(a), L1 and V1 are length and velocity calculations from diagram 1(d), L2 and V2 are length and velocity calculations from diagrams 1(d) plus 2(d).

$$T_{1d} = \langle \bar{k} | \frac{\partial}{\partial z} | 1s \rangle, \quad (18)$$

$$T_{2d} = \sum_{k_1 k_2} \langle 1s | \frac{\partial}{\partial z} | k_1 \rangle \langle \bar{k} | k_2 \rangle \langle k_1 k_2 | V | 1s 1s \rangle / (2\epsilon_{1s} - \langle 1s 1s | V | 1s 1s \rangle - \epsilon_{k_1} - \epsilon_{k_2}),$$

$$\sigma_k = 1.0271 \times 10^{-17} \text{ cm}^2 \frac{1}{k(\bar{\epsilon}_k - \epsilon_{1s})} |T_{1d} + T_{2d}|^2, \quad (20)$$

where we have neglected the correction to the ionization potential discussed in Sec. II.

IV. RESULTS AND DISCUSSIONS

The result of the present calculation by dipole-velocity formula is shown in Fig. 4. The dot-dash curve is from the experiment of Samson.⁶ Curve 1 is the result of the zeroth-order diagram Fig. 1(a) alone. The considerable deviation from experiment implies that the one-particle picture is inadequate. Curve 2 is the result of Fig. 1(d) which takes into account the final-state corrections but neglects the initial-state correction. The resulting curve 2 is seen to overcorrect the cross section and must be counterbalanced by the initial-state correlation given by Fig. 2(d). Our final result is in good agreement with experiment. It

also compared well with the best conventional theoretical result such as the dipole-length calculation of Stewart and Webb.¹¹

Cross sections by dipole length and velocity formulas are compared in Fig. 5. Since the Hamiltonian is local in Eq. (13), we have the relation

$$\left\langle q' \left| \frac{\partial}{\partial z} \right| q \right\rangle = (\epsilon_q - \epsilon_{q'}) \langle q' | z | q \rangle, \quad (21)$$

and there is no length-velocity difference in the zeroth-order cross section σ_0 .

Using Eq. (21), the length and velocity expressions T_{1b}^L and T_{1b}^V , respectively, of Fig. 1(b) have the relation

$$T_{1b}^V = \sum_{k'} \langle k, 1s | V | 1s, k' \rangle \langle k' | z | 1s \rangle - \omega T_{1b}^L, \quad (22)$$

where $\omega = \epsilon_k - \epsilon_{1s}$ is the photon energy in our approximation. Similarly, we have the following relation between the length and velocity expression of Fig. 2(a):

$$T_{2a}^V = - \sum_{k'} \langle k, k' | V | 1s, 1s \rangle \langle 1s | z | k' \rangle - \omega T_{2a}^L. \quad (23)$$

Thus we see that each of the above diagrams has the same amount of the length-velocity difference with opposite sign and, therefore, there is no length-velocity difference in the first-order BG calculation.

Because of the complete summation of intrashell correlation, Eq. (17) has nonlocal potential, and there is a large length-velocity difference between the cross sections from Fig. 1(d) as shown by curves L1 and V1 in Fig. 5. This difference is mainly from the first-order diagram Fig. 1(b), which is cancelled by that from Fig. 2(a), and it indeed becomes small in our final result L2 and V2.

The present work demonstrated that the use of multiple basis sets is not only desirable but necessary in dealing with problems such as the intrashell-consistency effects. It also results in a great calculational simplification, as exemplified by the mere two diagrams in this evaluation. The method is shown to be capable of yielding accurate results. The BG approach, together with the use of the multiple basis set should provide a powerful method in calculating general photoionization problems.

*Work partially supported by NASA and NSF.

†Formerly R. T. Pu.

¹H. P. Kelly, Phys. Rev. **136**, B896 (1964); **131**, 684 (1963); **144**, 39 (1966); see also, O. Sinançlı and K. A. Brueckner, *Three Approaches to Electron Correlation in Atoms* (Yale U.P., New Haven, 1970).

²R. T. Pu and E. S. Chang, Phys. Rev. **151**, 31 (1966); E. S. Chang, R. T. Pu, and T. P. Das, *ibid.* **174**, 1 (1968).

³N. C. Dutta, T. Ishihara, C. Matsubara, and T. P. Das, Phys. Rev. Letters **22**, 8 (1969); Phys. Rev. A **1**, 561 (1970).

⁴E. S. Chang and M. W. C. McDowell, Phys. Rev. **176**, 126 (1968).

⁵T. Ishihara and R. T. Poe, *Proceedings of the Sixth International Conference on the Physics of Electronic and Atomic Collisions* (MIT Press, Cambridge, Mass., 1969).

⁶J. A. R. Samson, J. Opt. Soc. Am. **54**, 876 (1964).

⁷T. Ishihara and R. T. Poe, Bull. Am. Phys. Soc. **915**, 1522 (1970); preceding paper, Phys. Rev. A **6**, 116 (1972).

⁸P. Nozières, *Theory of Interacting Fermi Systems* (Benjamin, New York, 1964).

⁹This correction has been neglected in the present

calculation. Detailed discussions will be given in the forthcoming paper.

¹⁰J. Goldstone, Proc. Roy. Soc. (London) **A239**, 267 (1957).

¹¹A. L. Stewart and T. G. Webb, Proc. Phys. Soc. (London) **82**, 532 (1963).

D Autoionization States of He and H⁻

A. K. Bhatia

*National Aeronautics and Space Administration, Goddard Space Flight Center,
Greenbelt, Maryland 20771*

(Received 9 March 1972)

Positions of the lowest ^{1,3}D^o autoionization states of He and H⁻ below the $n=2$ level of He⁺ and H have been calculated variationally using Feshbach's Q -operator formalism. The trial wave function is of the Hylleraas type with appropriate angular momentum factors. The widths and the shifts of the states have also been calculated. The shifts are found to be positive for all the states calculated here. The results with 112 terms for most states are lower than any previously calculated. The calculated lowest autoionization states of He and H⁻ (relative to the ground states of He and H, respectively) are 59.902 and 10.1185 eV, in good agreement with the observed values of 59.9 and 10.13 ± 0.015 eV.

I. INTRODUCTION

A number of resonances¹ have been observed in He and H⁻ below the threshold of He⁺ and H. Feshbach's Q -operator formalism has been applied successfully to calculate^{2,3} the positions and the widths of the S and P autoionization states. The purpose of this paper is to extend these calculations to the D autoionization states in He and H⁻ observed below the $n=2$ threshold of the respective targets. These states lie in the continuum of electron scattering from the single-electron target

system. They are not the stationary states of the two-electron Hamiltonian, and they autoionize by electron emission leaving behind bound states of the single-electron system. The energy of the state can be written as⁴

$$E = \mathcal{E}_Q + \Delta_Q, \quad (1)$$

where \mathcal{E}_Q is calculated variationally and Δ_Q is the shift of \mathcal{E}_Q due to the interaction of the discrete state with the continuum.

The most general D -state wave function of even parity of two electrons⁵ is

$$\Phi(\vec{r}_1, \vec{r}_2) = (f \pm \tilde{f}) [-\mathcal{D}_2^{0*}(\theta, \phi, \psi) + \sqrt{3}(\cos\theta_{12})\mathcal{D}_2^{2*}(\theta, \phi, \psi)] + (f \mp \tilde{f}) \sqrt{3}(\sin\theta_{12})\mathcal{D}_2^{2*}(\theta, \phi, \psi) \\ + (g \pm \tilde{g}) [-\cos\theta_{12}\mathcal{D}_2^{0*}(\theta, \phi, \psi) + \sqrt{3}\mathcal{D}_2^{2*}(\theta, \phi, \psi)] \quad (2)$$

where \mathcal{D} are the rotational harmonics, depending on the symmetric Euler angles θ, ϕ, ψ .⁵ These functions are eigenfunctions of exchange; indicating that they satisfy the following property;

$$\mathcal{E}_{12} \mathcal{D}_l^{k*} = \pm (-1)^{l+k} \mathcal{D}_l^{k*}. \quad (3)$$

The trial wave function is of Hylleraas type when the radial functions $f=f(r_1, r_2, r_{12})$ and $g=g(r_1, r_2, r_{12})$ are given by

$$f(r_1, r_2, r_{12}) = e^{-(\gamma_1 r_1 + \delta_1 r_2)} r_2^2 \\ \times \sum_{l \geq 0} \sum_{m \geq 0} \sum_{n \geq 0} C_{lmn}^{(1)} r_1^l r_2^m r_{12}^n, \quad (4a)$$

$$g(r_1, r_2, r_{12}) = e^{-(\gamma_2 r_1 + \delta_2 r_2)} r_1 r_2$$

$$\times \sum_{l \geq 0} \sum_{m \geq 0} \sum_{n \geq 0} C_{lmn}^{(2)} r_1^l r_2^m r_{12}^n. \quad (4b)$$

It is implied in Eq. (2) that

$$\tilde{f} = f(r_2, r_1, r_{12}) \quad (5a)$$

and

$$\tilde{g} = g(r_2, r_1, r_{12}). \quad (5b)$$

Using properties (3) and (5) in Eq. (2), we see that the wave function is manifestly space symmetric (upper sign) or space antisymmetric (lower sign). The space-symmetric and antisymmetric solutions correspond to singlet and triplet states, respectively.

To the best of our knowledge, this is the first